Journal of Cardiovascular Magnetic Resonance®, 3(4), 331–338 (2001)

Scan Reproducibility of Magnetic Resonance Imaging Assessment of Aortic Atherosclerosis Burden

Stephen K. Chan,[1] Farouc A. Jaffer,[1,3] Rene M. Botnar,[1,4] Kraig V. Kissinger,[1] Lois Goepfert,[1] Michael L. Chuang,[1] Christopher J. O'Donnell,[3,5] Daniel Levy,[1,5] and Warren J. Manning[1,2]

[1]Harvard-Thorndike Laboratory of the Department of Medicine (Cardiovascular Division), Beth Israel Deaconess Medical Center, Boston, Massachusetts
[2]Harvard-Thorndike Laboratory of the Department of Radiology, Beth Israel Deaconess Medical Center, Boston, Massachusetts
[3]Department of Medicine (Cardiology Division), Massachusetts General Hospital, Boston, Massachusetts
[4]Philips Medical Systems (RMB), Best, The Netherlands
[5]National Heart, Lung, and Blood Institute's Framingham Heart Study, Framingham, Massachusetts

ABSTRACT

Subclinical atherosclerosis precedes the onset of clinical disease by many years. Noninvasive magnetic resonance imaging (MRI) offers the opportunity to visualize and quantify atherosclerotic plaque. However, the reproducibility of MRI measurements of abdominal and thoracic aortic atherosclerosis has not been reported. Electrocardiogram-gated, T2-weighted, turbo spin echo MRI of the descending thoracic and abdominal aorta was performed on 16 subjects, comprising 10 subjects with multivessel coronary artery disease (CAD) and 6 subjects without angiographic CAD. Three identical MRIs were performed on each subject, with subject repositioning between the second and third scans. Aortic anatomic and plaque measurements were performed in a blinded fashion. Fourteen subjects (88%) had MRI evidence of atherosclerotic plaque on at least one image. Slice plaque burden, plaque area,

Address correspondence and reprint requests to Warren J. Manning.

and plaque perimeter were greater in the CAD group (52% vs. 9%, $p = 0.002$*; 264 vs. 18 mm*^{2}, $p = 0.009$*; 159 vs. 15 mm,* $p = 0.006$*, respectively). Measurements of total aortic lumen area, lumen circumference, plaque area, and plaque perimeter correlated highly among the three scans (all* $r = 0.96$*, all* $p < 0.001$*). Measurements of slice-specific aortic lumen area and lumen circumference also correlated highly (all* $r = 0.98$*, all* $p < 0.001$*). Correlations of slice-specific plaque area and plaque perimeter were significant (all* $p < 0.001$*) but less robust (*$r = 0.62–0.85$*). These data demonstrate that MRI is a reproducible technique for assessing aortic anatomy and total aortic atherosclerosis, but increased slice density should be considered if serial evaluation of slice-specific data is desired.*

Key Words: *Aorta; Atherosclerosis; Magnetic resonance imaging; Subclinical disease*

INTRODUCTION

Atherosclerosis, leading to stroke and coronary artery disease (CAD), is a major cause of morbidity and mortality in the United States. There is increasing evidence that the primary mechanism for stroke and acute coronary syndromes is disruption of an atherosclerotic plaque with superimposed thrombosis (1,2). Subclinical atherosclerosis precedes the onset of clinically apparent disease (e.g., angina, myocardial infarction, or stroke) by many years or decades (3,4). Aortic atherosclerosis predicts clinical CAD and CAD events (5,6). Autopsy data in young persons dying of trauma suggest that subclinical atherosclerosis is associated with traditional CAD risk factors (7). Conventional x-ray angiography is poorly predictive of the sites of subsequent clinical events and underestimates underlying plaque burden (8–10). In addition, early in the development of coronary atherosclerosis, compensatory lumen enlargement, whereby the arterial wall initially expands in response to atherosclerotic plaque, results in relative preservation of lumen area despite significant plaque burden (11).

Magnetic resonance imaging (MRI) is a noninvasive technique that allows quantification and characterization (12–14) of atherosclerotic plaque. MRI has also been shown to provide anatomic information regarding thoracic aortic plaque that compares favorably with transesophageal echocardiography (15). MRI may therefore provide a means to observe the natural progression or regression of atherosclerosis in response to therapy (16). To our knowledge, however, the reproducibility of MRI measurements of aortic atherosclerosis burden has not been reported. This was the primary purpose of our study.

MATERIALS AND METHODS

MRI of the abdominal and thoracic aorta was performed on 16 adult subjects (12 men and 4 women aged 63 ± 9 years; range, 47–80 years). Ten subjects had a history of multivessel CAD, and 6 subjects had no evidence of CAD by recent (<1 year) x-ray coronary angiography. All subjects were in sinus rhythm and without contraindications to MRI. Written informed consent was obtained from all subjects, and the study was approved by the hospital Committee on Clinical Investigations.

MRI was performed using a commercial 1.5-T whole-body MR system (Gyroscan NT, Philips Medical Systems, Best, The Netherlands) with PowerTrak 6000 gradient system (23 mT/m, 220 μsec rise time). Twenty-four transverse 5-mm-thick (10-mm gap) images of the aorta extending from the arch to the distal bifurcation were obtained using an electrocardiogram-gated, T2-weighted, turbo spin echo sequence (TSE factor = 14) with fat saturation. Imaging parameters included an echo time of 45 msec, repetition time of three heart beats, and 264×330 mm field of view with 256×512 acquisition matrix resulting in an in-plane spatial resolution of 1.03×0.64 mm. To ensure signal void (from flowing blood) within the aortic lumen, time delays of 75 msec and 125 msec after the QRS were used for imaging of the thoracic and abdominal aorta, respectively. Fat saturation prepulses were used to suppress signal from fatty tissue contiguous to the aorta and to minimize chemical shift artifacts related to periadventitial fat. All data were acquired with prospective electrocardiogram gating during free breathing with four averages (thoracic aorta five-element cardiac synergy coil as radiofrequency receiver) or six averages (abdominal aorta body coil as radiofrequency receiver), both with foldover suppression.

Three identical MRIs were performed on each subject. The first two scans were performed in succession without any gross subject movement. After the second scan, the subject was removed from the scanner table, repositioned, and a third scan was performed with the most superior slice positioned at the aortic arch. Total imaging time for each scan was ~16 min. Total imaging time for each subject was ~90 min.

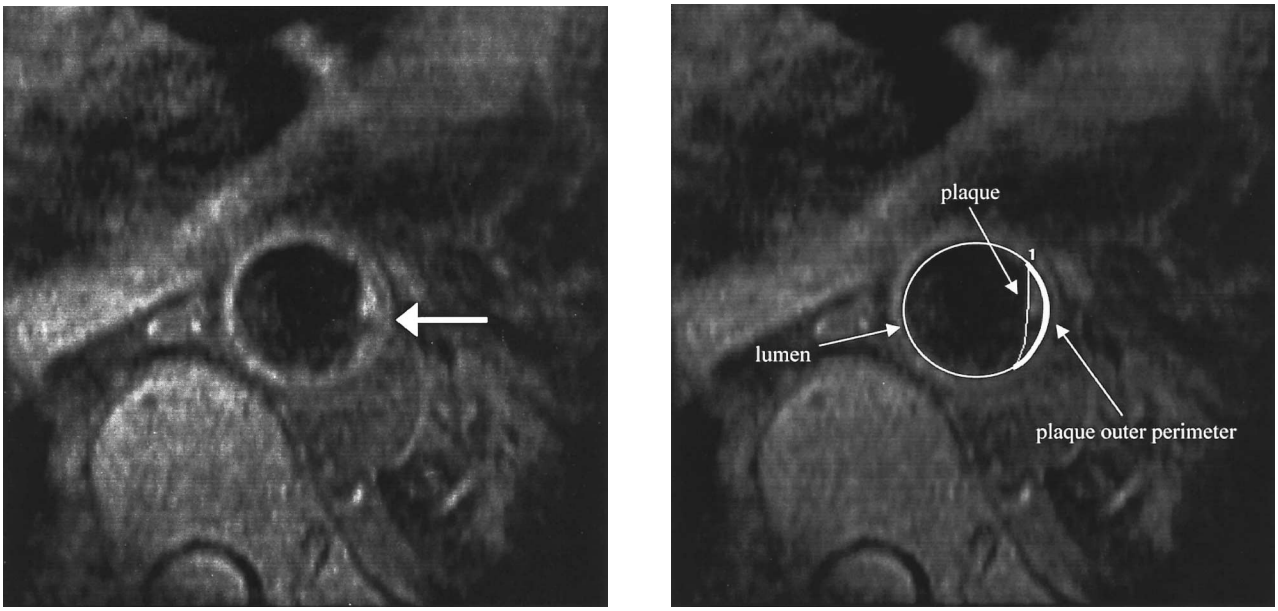

Figure 1. (a) Electrocardiogram-gated, T2-weighted, turbo spin echo, transverse magnetic resonance image of descending thoracic aorta in one subject with aortic plaque (white arrow). (b) Planimetry of aortic lumen for measurement of lumen area and lumen circumference, and planimetry of atherosclerotic plaque for measurement of plaque area and plaque outer perimeter. The outer surface of the plaque represents the plaque outer perimeter.

Images were transferred to a commercial EasyVision 4.0 workstation (Philips Medical Systems) for analysis. Images containing aortic lumen were designated as either thoracic or abdominal aorta, defined by their location above or below the diaphragm, respectively. In each image, the aortic lumen was manually planimetered using an interactive track-ball system and ellipsoid model to determine the cross-sectional area and circumference (Fig. 1). Each slice was then visually inspected for the presence of atherosclerotic plaques. Atherosclerotic plaques were defined as luminal protrusions with characteristic appearances on T2-weighted images (12–14) that were not obscured by chemical shift artifact, flow artifact from residual blood signal, or cardiac or respiratory motion artifact. For each plaque, the plaque outer perimeter and cross-sectional plaque area were recorded (Fig. 1). The plaque outer (rather than total) perimeter was measured so as to be analogous to autopsy surface area data

Table 1

Summary of Clinical and Aortic Data

	Total	CAD	No CAD	*p*
Number of subjects	16	10	6	
Age (yr)	63.4 ± 9.4	65.5 ± 7.6	60.0 ± 11.8	0.27
Aortic volume (cm^3)	107 ± 34	114 ± 39	97 ± 23	0.34
Aortic volume/height (cm^3/m)	62.3 ± 18.7	65.8 ± 21.8	56.4 ± 11.5	0.35
Aortic volume/BSA (cm^3/m^2)	54.6 ± 14.7	57.9 ± 17.4	49.1 ± 7.0	0.26
Slice-specific lumen area (mm^2)	339 ± 135	361 ± 144	298 ± 106	<0.001
Slice-specific lumen circumference (mm)	64.1 ± 13.2	66.1 ± 13.8	60.3 ± 11.3	<0.001
Slice plaque burden (%)	35.4 ± 30.1	51.6 ± 27.0	8.5 ± 9.5	0.002
Total plaque area (mm^2)	172 ± 194	264 ± 194	18 ± 20	0.009
Total plaque perimeter (mm)	105 ± 109	159 ± 105	15 ± 17	0.006

BSA, body surface area.

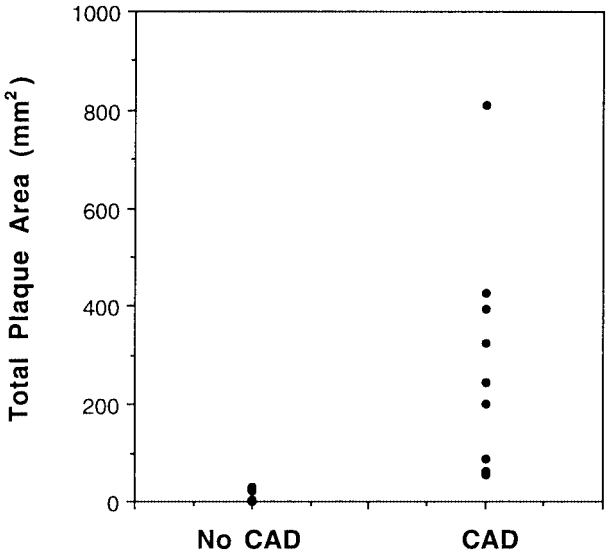

Figure 2. Individual subject data for total plaque area in those with multivessel CAD and those without CAD.

(4). The aortic volume was calculated as the sum of the aortic lumen areas multiplied by 15 mm (sum of the slice thickness and slice gap). Aortic lumen area from slices with poor image quality were estimated using linear interpolation from adjacent slice data. Images were analyzed in random order and by an experienced observer blinded to all clinical data.

Statistical Analysis

All data are presented as means ± SD. For each scan, total and slice-specific aortic lumen area, aortic lumen circumference, plaque area, and plaque outer perimeter were determined. The aortic bifurcation and diaphragm were used as anatomic landmarks for alignment of slice-specific data. Slice plaque burden (number of slices with plaque/total number of slices) was also determined. Total and slice-specific data among the three scans were compared by repeated-measures analysis of variance. Least-squares linear regression was used to assess the relationship between the scans, which were summarized using the Pearson correlation coefficient (r). Bland-Altman analysis was used to evaluate the agreement between studies. All analyses were two-tailed, with $p = 0.05$ considered significant.

RESULTS

All subjects completed MRI without complications. Clinical and aortic data are summarized in Table 1. Fourteen subjects (88%) had evidence of aortic atherosclerotic plaque on at least one image. Slice plaque burden was greater in those with CAD compared with those without CAD with over half of aortic slices containing plaque in the CAD group ($p = 0.002$). Total plaque area ($p = 0.009$, Fig. 2) and plaque outer perimeter ($p = 0.006$) were also greater in the CAD group, with minimal overlap between groups. Mean aortic lumen area and lumen circumference were greater in the CAD group (both $p < 0.001$) with a trend toward larger aortic volume in the CAD group.

Among the three MRIs performed on each subject, measurements of total aortic lumen area, lumen circumference, plaque area, and plaque outer perimeter were all highly correlated (all $r = 0.96$, all $p < 0.001$; Table 2, Fig. 3). Measurements of slice-specific aortic lumen area and lumen circumference also correlated highly (all $r = 0.98$, all $p < 0.001$; Table 2). Correlations of slice-specific plaque area and plaque outer perimeter were significant (all $p < 0.001$) but less robust ($r = 0.62$–0.85;

Table 2

Summary of Correlation (r Values) of Aortic Lumen and Plaque Measurements Among the Three MRI

	Scan 1 vs. Scan 2	Scan 1 vs. Scan 3	Scan 2 vs. Scan 3
Total lumen area (mm^2)	0.99	0.99	0.99
Total lumen circumference (mm)	0.99	0.99	0.99
Total plaque area (mm^2)	0.98	0.97	0.99
Total plaque perimeter (mm)	0.98	0.96	0.98
Slice-specific lumen area (mm^2)	0.99	0.98	0.98
Slice-specific lumen circumference (mm)	0.99	0.98	0.98
Slice-specific plaque area (mm^2)	0.85	0.73	0.62
Slice-specific plaque perimeter (mm)	0.85	0.76	0.68

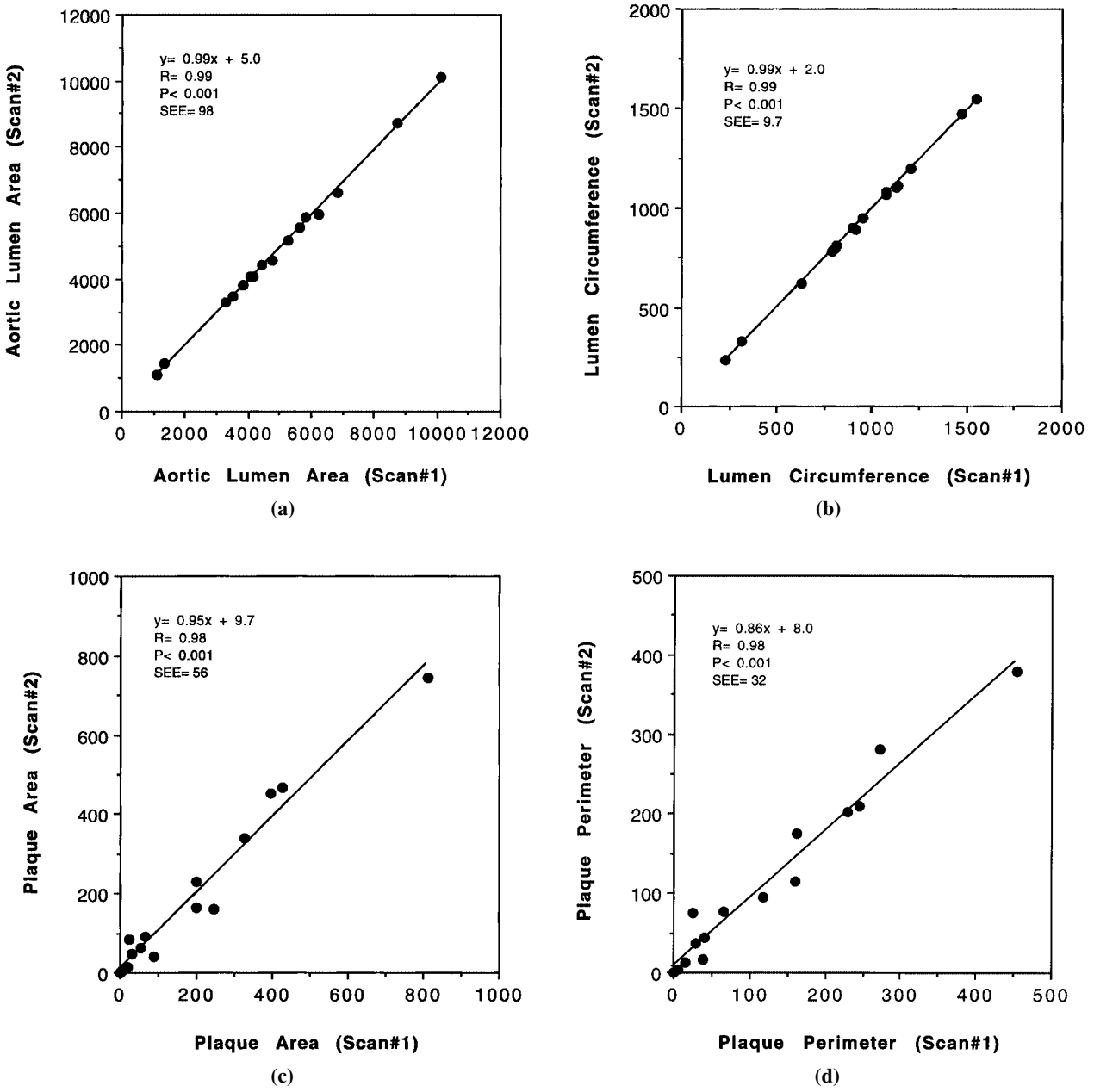

Figure 3. (a) Graph of total aortic lumen area determined from scan 1 and scan 2. (b) Graph of total aortic lumen circumference determined from scan 1 and scan 2. (c) Graph of total plaque area determined from scan 1 and scan 2. (d) Graph of total plaque outer perimeter determined from scan 1 and scan 2. The lines represent the best fit as determined by least-squares linear regression.

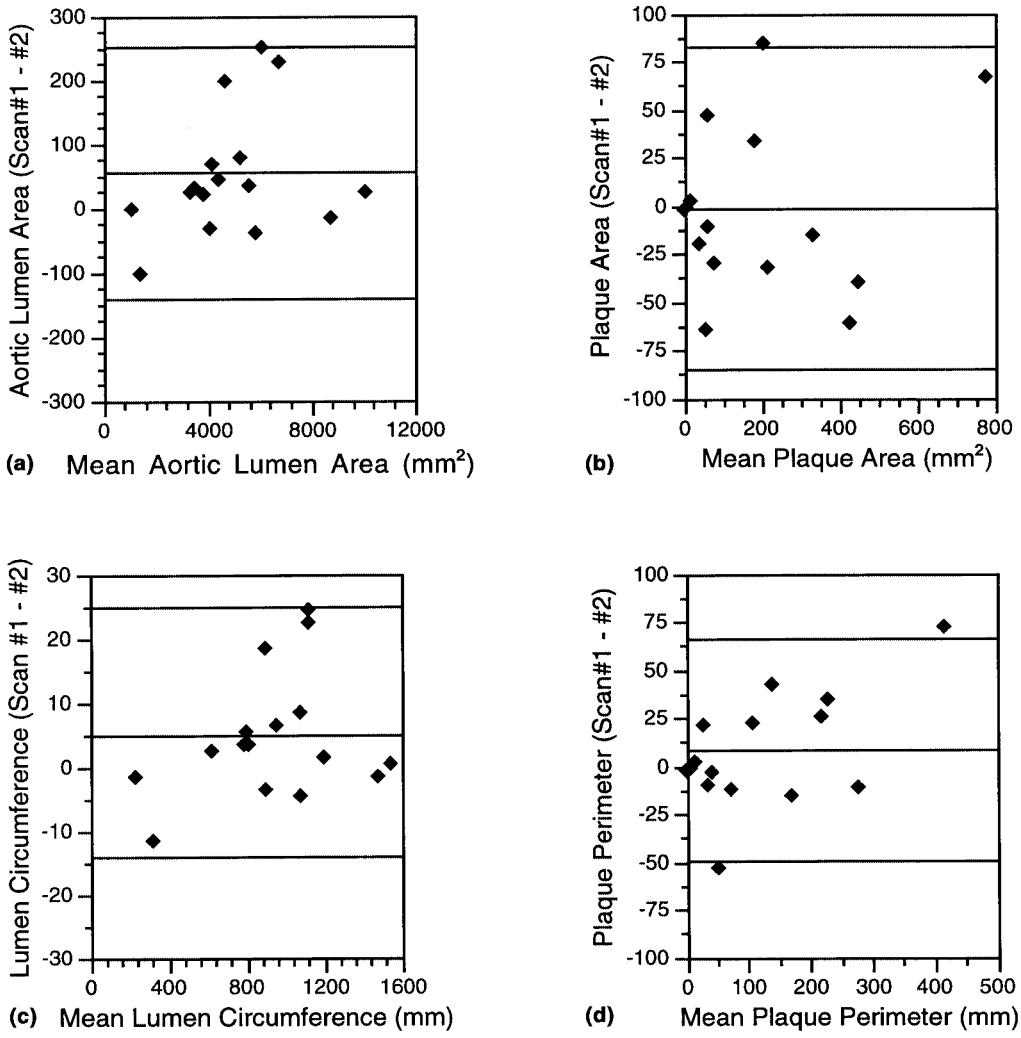

Figure 4. Bland-Altman comparisons of measurements determined from scan 1 and scan 2 of (a) total aortic lumen area, (b) total lumen circumference, (c) total plaque area, and (d) total plaque outer perimeter.

Table 2). Bland-Altman analyses for aortic lumen and plaque measurements are presented in Fig. 4.

DISCUSSION

Noninvasive MRI assessment of aortic atherosclerosis has been proposed as an important clinical and epidemiologic tool for assessment of clinical and subclinical disease (17,18), but the reproducibility of MRI data has not been previously reported. In this study, we validate the use of MRI as a highly reproducible method for assessing both aortic cross-sectional anatomy and total aortic atherosclerotic plaque burden. Slice-specific measurements of aortic plaque burden were significant but less robust, likely related to the relatively wide (10-mm) slice gap in the study protocol. Thus, if slice-specific regression or progression studies are desired, increased slice density (smaller interslice gap) should be considered.

Although the primary purpose of this study was not to investigate differences in aortic anatomy and plaque burden among subjects with and without CAD, we found that both total aortic plaque area and slice plaque burden were increased among those with multivessel CAD. Also, the average cross-sectional aortic lumen area and circumference were significantly greater among those with

CAD. These data are provocative because they support a ''Glagov effect'' (11) in the aorta. Whether or not such compensatory enlargement in response to atherosclerosis actually occurs in the human aorta has yet to be shown.

Our findings regarding the reproducibility of MRI in assessing aortic anatomy and atherosclerotic plaque burden are of primary importance in establishing the usefulness of this test, both for investigative and clinical applications. MRI is currently the only noninvasive method of directly visualizing and quantifying thoracic and abdominal aortic atherosclerotic plaque. MRI holds the potential of detecting the presence of atherosclerotic plaque before it becomes clinically significant and may be suitable for monitoring the regression or progression of atherosclerotic disease after therapy. Studies are already underway to determine the clinical predictive utility of MRI screening of asymptomatic aortic atherosclerosis (17,18). The current study fulfills a critical step of demonstrating the integrity of MRI as a reproducible imaging tool for quantifying aortic atherosclerosis.

In this study, we sought to determine the reproducibility of MRI measurements of aortic atherosclerosis burden by performing serial studies without patient movement and following patient removal from the MR environment and subsequent scanning. Other potentially important variables, such as comparisons with different MR pulse sequences, MR vendor platforms, set-up/scanning by different MR technologists, and scanning on a different day or time of day, were not investigated and remain to be examined. Finally, a more specific positioning landmark for the imaging volume (e.g., ostium of a renal artery) may have facilitated improved slice-specific reproducibility.

CONCLUSIONS

MRI measurements of total aortic and slice-specific area and circumference are highly reproducible. MRI measurements of total plaque area and perimeter also correlate highly, but the correlation of slice-specific plaque data is less robust, likely due to the slice gaps and reduced slice density in the protocol used. These data demonstrate that MRI is a reproducible technique for assessing total aortic atherosclerosis, but increased slice density should be considered if serial evaluation of slice-specific data is desired.

REFERENCES

1. Falk, E.; Shah, P.; Fuster, V. Coronary Plaque Disruption. Circulation **1995**, *92*, 657–671.
2. Libby, P.; Schoenbeck, U.; Mach, F.; Selcoyn, A.P.; Ganz, P. Current Concepts in Cardiovascular Pathology: the Role of LDL Cholesterol in Plaque Rupture and Stabilization. Am. J. Med. **1998**, *104*, S14–S18.
3. Relationship of Atherosclerosis in Young Men to Serum Lipoprotein Cholesterol Concentrations and Smoking. A preliminary report from the Pathobiological Determinants of Atherosclerosis in Youth (PDAY) Research Group. JAMA **1990**, *264*, 3018–3024.
4. Tracy, R.E.; Newman, W.P.; Wattigney, W.A.; Berenson, G.S. Risk Factors and Atherosclerosis in Youth Autopsy Findings of the Bogalusa Heart Study. Am. J. Med. Sci. **1995**, *310*, S37–S41.
5. Fazio, G.P.; Redberg, R.F.; Winslow, T.; Schiller, N.B. Transesophageal Echocardiography Detected Atherosclerotic Aortic Plaque Is a Marker for Coronary Artery Disease. J. Am. Coll. Cardiol. **1993**, *21*, 144–150.
6. Witteman, J.C.; Kannel, W.B.; Wolf, P.A.; Grobbee, D.E.; Hofman, A.; D'Agostino, R.B.; Cobb, J.C. Aortic Calcified Plaques and Cardiovascular Disease (The Framingham Study). Am. J. Cardiol. **1990**, *66*, 1060–1064.
7. Pathobiological Determinants of Atherosclerosis in Youth (PDAY) Research Group. Natural History of Aortic and Coronary Atherosclerosis Lesions in Youth. Findings from the PDAY Study. Arterioscler. Thromb. **1993**, *13*, 1291–1298.
8. Brown, B.G.; Gallery, C.A.; Badger, R.S.; Kennedy, J.W.; Mathey, D.; Bolson, E.L.; Dodge, H.T. Incomplete Lysis of Thrombus in the Moderate Underlying Atherosclerotic Lesion During Intracoronary Infusion of Streptokinase for Acute Myocardial Infarction: Quantitative Angiographic Observations. Circulation **1986**, *773*, 653–661.
9. Little, W.C.; Constantinescu, M.; Applegate, R.J.; Kutcher, M.A.; Burrows, M.T.; Kahl, F.R.; Santamore, W.P. Can Coronary Angiography Predict the Site of a Subsequent Myocardial Infarction in Patients With Mild-To-Moderate Coronary Artery Disease? Circulation **1988**, *78*, 1157–1166.
10. Ambrose, J.A.; Winters, S.L.; Stern, A.; Eng, A.; Teichhotz, L.F.; Gorlin, R.; Fuster, V. Angiographic Morphology and the Pathogenesis of Unstable Angina Pectoris. J. Am. Coll. Cardiol. **1988**, *12*, 56–62.
11. Glagov, S.; Weisenberg, E.; Zarins, C.K.; et al. Compensatory Enlargement of Human Atherosclerotic Coronary Arteries. N. Engl. J. Med. **1987**, *316*, 1371–1375.
12. Toussaint, J.F.; LaMuraglia, G.M.; Southern, J.F.; Fuster, V.; Kantor, H.L. Magnetic Resonance Images Lipid, Fibrous, Calcified, Hemorrhagic, and Thrombotic Components of Human Atherosclerosis In Vivo. Circulation **1996**, *94*, 932–938.
13. Rogers, W.J.; Prichard, J.W.; Hu, Y.L.; Olson, P.R.; Benckart, D.H.; Kramer, C.M.; Vido, D.A.; Reichek, N. Characterization of Signal Properties in Atherosclerotic Plaque Components by Intravascular MRI. Arterioscler. Thromb. Vasc. Biol. **2000**, *20*, 1824–1830.
14. Hatsukami, T.S.; Ross, R.; Polissar, N.L.; Yuan, C. Visu-

alization of Fibrous Cap Thickness and Rupture in Human Atherosclerotic Carotid Plaque In Vivo With High Resolution Magnetic Resonance Imaging. Circulation **2000**, *102*, 959–964.

15. Fayad, Z.A.; Nahar, T.; Fallon, J.T.; Goldman, M.; Aguinaldo, J.G.; Badimon, J.J.; Shinnar, M.; Chesebro, J.H.; Fuster, V. In Vivo Magnetic Resonance Evaluation of Atherosclerotic Plaques in the Human Thoracic Aorta; A Comparison With Transesophageal Echocardiography. Circulation **2000**, *101*, 2503–2509.
16. Corti, R.; Badimon, J.J.; Worthley, S.G.; Helft, G.; Fayad, Z.A.; Fuster, V. Statin Therapy Reduces Burden in Human Atherosclerotic Lesions: Longitudinal Study Using Noninvasive MRI (abstract). Circulation **2000**, *102*, II-459.
17. Jaffer, F.A.; O'Donnell, C.J.; Chan, S.K.; Kissinger, K.V.; Levy, D.; Manning, W.J. A New MRI Index of Aortic Atherosclerotic Burden in a Healthy Population (abstract). Circulation **1999**, *100*, I-521.
18. Jaffer, F.A.; O'Donnell, C.J.; Larson, M.; Kissinger, K.V.; Chan, S.K.; Botnar, R.; Edelman, R.R.; Levy, D.; Manning, W.J. MRI Assessment of Aortic Atherosclerosis in an Asymptomatic Population: the Framingham Heart Offspring MRI Pilot Study (abstract). Circulation **2000**, *102*, II-458.

Received January 19, 2001
Accepted May 10, 2001

MARCEL DEKKER, INC.
270 Madison Avenue, New York, New York 10016